

SCIENTIFIC REPORTS



OPEN

Manassantin B shows antiviral activity against coxsackievirus B3 infection by activation of the STING/TBK-1/IRF3 signalling pathway

Jae-Hyoung Song¹, Jae-Hee Ahn¹, Seong-Ryeol Kim¹, Sungchan Cho³, Eun-Hye Hong¹, Bo-Eun Kwon¹, Dong-eun Kim³, Miri Choi³, Hwa-Jung Choi⁴, Younggil Cha¹, Sun-Young Chang¹ & Hyun-Jeong Ko¹

Coxsackievirus B3 (CVB3) is an important human pathogen associated with the development of acute pancreatitis, myocarditis, and type 1 diabetes. Currently, no vaccines or antiviral therapeutics are approved for the prevention and treatment of CVB3 infection. We found that *Saururus chinensis* Baill extract showed critical antiviral activity against CVB3 infection *in vitro*. Further, manassantin B inhibited replication of CVB3 and suppressed CVB3 VP1 protein expression *in vitro*. Additionally, oral administration of manassantin B in mice attenuated CVB3 infection-associated symptoms by reducing systemic production of inflammatory cytokines and chemokines including TNF- α , IL-6, IFN- γ , CCL2, and CXCL-1. We found that the antiviral activity of manassantin B is associated with increased levels of mitochondrial ROS (mROS). Inhibition of mROS generation attenuated the antiviral activity of manassantin B *in vitro*. Interestingly, we found that manassantin B also induced cytosolic release of mitochondrial DNA based on cytochrome C oxidase DNA levels. We further confirmed that STING and IRF-3 expression and STING and TBK-1 phosphorylation were increased by manassantin B treatment in CVB3-infected cells. Collectively, these results suggest that manassantin B exerts antiviral activity against CVB3 through activation of the STING/TBK-1/IRF3 antiviral pathway and increased production of mROS.

The family *Picornaviridae* is currently divided into 35 genera, three of which are important causes of human infectious diseases¹. Coxsackievirus B3 (CVB3) is included in the genus *Enterovirus* within the family *Picornaviridae* and is a major causative agent of cardiac muscle infection^{2–4}. In addition, CVB3 occasionally causes chronic pancreatic inflammatory diseases resulting in insulin-dependent type I diabetes mellitus and idiopathic chronic pancreatitis^{4–6}. However, specific clinical therapy is not presently available for this virus type, although a number of antiviral candidates are under development⁷.

Medicinal plants—with often manifold targets, less severe side effects, low potential to cause drug tolerance, and low cost—are increasingly considered suitable alternative sources of antiviral candidates^{8–12}. *Saururus chinensis* Baill, a well-known medicinal plant of China and South Korea, has been traditionally used for the treatment of beriberi, hypertension, pneumonia, oedema, jaundice, leprosy, and gonorrhoea^{13,14}. *Saururus* chemical studies have revealed the presence of more than 20 lignans¹⁵, some of which exhibit neuroleptic¹⁶, hepatoprotective¹⁷, and antifeedant activities¹⁸. Additionally, *S. chinensis* Baill was reported to protect against sepsis¹⁵, cell adhesion¹⁹,

¹College of Pharmacy, Kangwon National University, Chuncheon, South Korea. ²Research Institute of Pharmaceutical Science and Technology (RIPST), College of Pharmacy, Ajou University, Suwon, South Korea. ³Anticancer Agent Research Center, Korea Research Institute of Bioscience & Biotechnology, Ochang, South Korea. ⁴Department of Beauty Science, Kwangju Women's University, Gwangju, South Korea. Jae-Hyoung Song and Jae-Hee Ahn contributed equally. Correspondence and requests for materials should be addressed to S.-Y.C. (email: sychang@ajou.ac.kr) or H.-J.K. (email: hjko@kangwon.ac.kr)

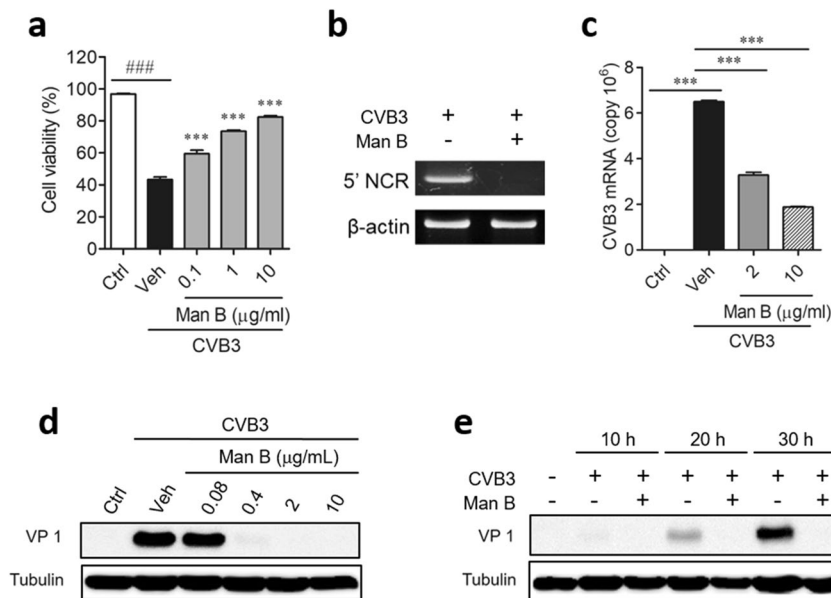


Figure 1. Antiviral activity of manassantin B against coxsackievirus B3 *in vitro*. **(a)** Vero cells were infected with coxsackievirus B3 (CVB3) at 50% cell culture infective dose (CCID₅₀) and treated with manassantin B (Man B). The cytopathic effect on virus-infected Vero cells was analysed 2 days after infection. The antiviral activity was calculated based on cell viability. **(b)** Replication of CVB3 in Vero cells at 48 h after infection with CVB3 in the presence of Man B (10 µg/mL) was detected by RT-PCR of the CVB3 genome. **(c)** Quantitative real-time PCR was conducted to measure the copy number of CVB3 viral RNA in Vero cells after treatment with Man B (2 and 10 µg/mL). **(d)** Western blotting was performed to determine the effect of different concentrations of Man B on the production of CVB3 VP1 protein. Vero cells (1×10^6) were seeded in a 6-well plate and incubated overnight. Cells were infected with CVB3 at an MOI of 0.8 and treated with 0.08, 0.4, 2, and 10 µg/mL of Man B. After 48 h, cells were harvested. **(e)** To evaluate the antiviral activity of Man B at multiple time points, cells were harvested at 10, 20, and 30 h after CVB3 infection and treatment with 2 µg/mL of Man B. Thirty micrograms of total cellular proteins from CVB3-infected Vero cells was electrophoresed and subjected to western blot. α -Tubulin was used as a loading control for each set of samples. The samples were derived from the same experiment, and the gels/blots were processed in parallel. Results are shown as means \pm SEM of 3 independent experiments. $###P < 0.001$ for comparison with non-infected control group (Ctrl); $***P < 0.001$ for comparison with CVB3-infected vehicle group (Veh), Bonferroni's multiple comparison test (ANOVA).

inflammation^{20,21}, and hypercholesterolemia²². Other types of compounds found in *S. chinensis* Baill include aris-tolactams, flavonoids, anthraquinones, and fruanoditerpenes^{23,24}.

In the current study, we found that *S. chinensis* Baill extract exerted significant antiviral activity against CVB3 infection in Vero cells and revealed manassantin B (Man B) as one of the antiviral components isolated from the ethyl acetate fraction of the *S. chinensis* Baill extract. Man B protected mice from systemic infection of CVB3 and reduced CVB3-mediated inflammatory cytokine production. Man B exerted antiviral activity against CVB3 through activation of the STING/TBK-1/IRF3 signalling pathway as well as increased production of mitochondrial ROS (mROS). This study may shed light on a medicinal plant whose extract or active compounds may be used clinically for the effective treatment of enterovirus infection.

Results

Man B from *S. chinensis* Baill extract showed antiviral activity against CVB3 *in vitro*. We found that the *S. chinensis* Baill extract showed antiviral activity against CVB3 *in vitro* during screening of antiviral candidates from medicinal plants. Both the hexane and ethyl acetate fraction of the methanol extract of *S. chinensis* Baill showed strong antiviral activity (Supplementary Table S1).

The ethyl acetate fraction was further fractionated using C18 column chromatography; Fr.10 showed the highest antiviral activity (Supplementary Table S2). We isolated one active compound from Fr.10, which was identified as Man B using UV spectroscopic, EI-MS, ¹H-NMR, and ¹³C-NMR analysis (Supplementary Fig. S1). Man B is a lignin compound known to exist in *S. chinensis* Baill²⁵. The interpretations of proton and carbon signals were consistent with those of Seo *et al.* (2009). Man B is a yellow amorphous powder characterised as follows: ESI-MS (70 eV), *m/z* (% relative intensity): 739.9 [M + Na]⁺, ¹H NMR (DMSO-*d*₆, 400 MHz), and ¹³C NMR (DMSO-*d*₆, 100 MHz) (Supplementary Table S3).

Man B inhibited the replication of CVB3 in Vero cells. To confirm the antiviral activity of Man B against CVB3, the effect of Man B on the viability of Vero cells infected with CVB3 was evaluated. Man B significantly blocked the CVB3-mediated cytotoxicity of Vero cells (Fig. 1a). In addition, CVB3 replication in Vero cells was inhibited by Man B as determined by RT-PCR (Fig. 1b) and quantitative real-time RT-PCR (Fig. 1c,

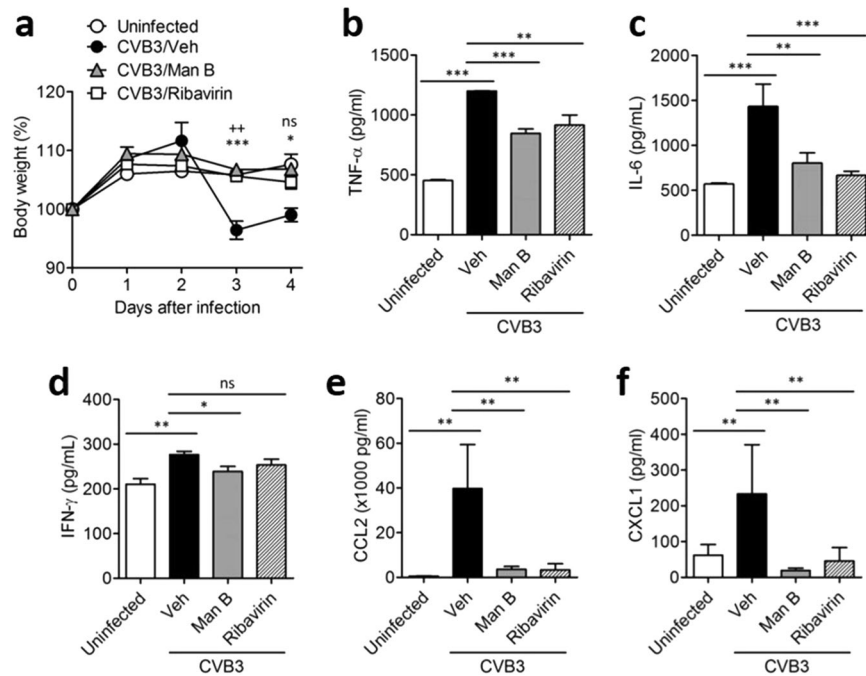


Figure 2. Antiviral activity of manassantin B against coxsackievirus B3 *in vivo*. BALB/c mice ($n = 5/\text{group}$) were intraperitoneally infected with a 1×10^6 pfu/100 μL of coxsackievirus B3 (CVB3) and administered manassantin B (Man B) (2.5 mg/kg), ribavirin (10 mg/kg), or vehicle (Veh) (0.5% carboxymethyl cellulose). (a) Body weight was measured for 5 days. Results are shown as means \pm SEM of 3 independent experiments. $^{++}P < 0.01$ for comparison with CVB3/Veh and CVB3/Ribavirin; $^*P < 0.05$, $^{***}P < 0.001$ for comparison with CVB3/Veh and CVB3/Man B, Bonferroni's multiple comparison test (ANOVA). Mice were infected with 1×10^6 pfu/100 μL of CVB3. After 5 days of infection, the level of chemokines and cytokines was analysed by ELISA. Levels of (b) TNF- α , (c) IL-6, (d) IFN- γ , (e) CCL2, and (f) CXCL-1 in serum isolated from control mice, vehicle-treated, CVB3-infected mice (Veh), manassantin B-treated, CVB3-infected mice, or ribavirin-treated, CVB3-infected mice. Data represent the mean values of five mice per group. Results are shown as means \pm SEM of 3 independent experiments. $^*P < 0.05$, $^{**}P < 0.01$, $^{***}P < 0.001$, Bonferroni's multiple comparison test (ANOVA).

Supplementary Fig. S2) of the CVB3 RNA genome. We also confirmed that CVB3 VP1 protein expression was completely suppressed by 0.4 $\mu\text{g}/\text{mL}$ Man B treatment through western blot analysis (Fig. 1d) and that Man B strongly suppressed viral replication and capsid protein production at the early stage of the virus life cycle (Fig. 1e). Therefore, we confirmed the antiviral activity of Man B against CVB3 infection *in vitro*. To determine whether the antiviral activities of Man B were restricted to CVB3, we investigated its antiviral activity against other coxsackieviruses including CVB1, CVB2, CVB4, CVB5, and CVB6 (Supplementary Fig. S3). Interestingly, Man B displayed significant antiviral activity against all tested group B coxsackieviruses with 50% inhibitory concentration (IC_{50}) values of 0.88–8.20 $\mu\text{g}/\text{mL}$ (Supplementary Table S4).

To evaluate whether Man B inhibits CVB3 replication, we conducted a time-of-drug addition assay. We found that the addition of Man B at 8 h after CVB3 infection did not show antiviral activity, suggesting that Man B plays an inhibitory role in the early period of CVB3 infection (Supplementary Fig. S4). To determine whether Man B directly affects viral protein translation, we performed an internal ribosome entry site (IRES) binding inhibition assay with an IRES dual reporter system²⁶. As a result, the ratio of Renilla luciferase activity, which reflects Cap-dependent translation to firefly luciferase activity, which reflects IRES translation was not significantly different between the vehicle- and Man B-treated groups. Thus, Man B did not appear to directly inhibit the viral IRES-dependent translation (Supplementary Fig. S5).

Man B reduced pro-inflammatory cytokines and chemokines in the serum of CVB3-infected mice. To assess whether Man B elicited antiviral activity *in vivo*, we adopted the pancreatic infection model of CVB3 as we previously reported²⁷. Intraperitoneal injection of 1×10^6 pfu CVB3 resulted in body weight loss of BALB/c mice, whereas daily injection of 2.5 mg/kg Man B or 10 mg/kg ribavirin for 4 days prevented body weight loss caused by CVB3 infection (Fig. 2a). Likewise, the level of serum cytokines and chemokines including TNF- α , IL-6, IFN- γ , CCL2, and CXCL-1, which increased after 5 days post CVB3 infection, was significantly reduced by treatment with Man B or ribavirin (Fig. 2b–f). Collectively, these results suggested that Man B ameliorated CVB3 infection-associated symptoms similarly to ribavirin.

Man B induced mitochondrial damage with mROS generation. Treatment of CVB3-infected Vero cells with Man B considerably increased the levels of mROS. Addition of the mitochondrial uncoupling agent

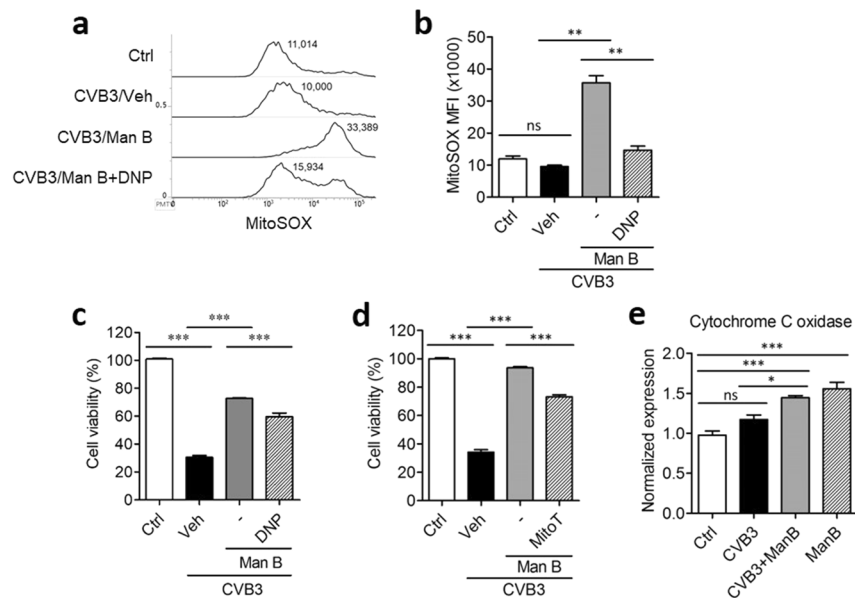


Figure 3. Manassantin B induced mitochondrial ROS and release of mitochondrial DNA into the cytosol. (a) Coxsackievirus B3 (CVB3)-infected Vero cells were treated with manassantin B (Man B) with or without 20 μ M 2,4-dinitrophenol (DNP). Harvested cells were stained with 5 μ M of MitoSOX reagent and analysed by fluorescence-activated cell sorting (FACS) to detect reduction in mitochondrial ROS. (b) The mean MitoSOX fluorescence index (MFI) was measured. (c) 50 μ M of DNP and (d) 50 μ M of mitoTempo (MitoT) were added to Man B-treated and CVB3-infected cells. (e) Cytosolic mitochondrial DNA was detected by PCR. Ctrl, control; Veh, vehicle. Data are presented as means \pm SEM of 5 independent experiments. * P < 0.05, ** P < 0.01, *** P < 0.001, Bonferroni's multiple comparison test (ANOVA).

2,4-dinitrophenol (DNP) reduced the generation of mROS following Man B treatment (Fig. 3a,b). In addition, treatment of CVB3-infected Vero cells with 50 μ M of DNP, a mitochondrial electron transport chain uncoupler, or mitoTempo, a mitochondria-targeted antioxidant, significantly inhibited the antiviral activity of Man B, albeit not completely (Fig. 3c,d).

We next assessed whether Man B also induced cytosolic release of mitochondrial DNA (mtDNA), since mtDNA was recently found to trigger innate antiviral signalling²⁸. For this, cytochrome C oxidase DNA was amplified from genomic DNA of the cytosolic fraction. As a result, Man B treatment increased cytosolic cytochrome C oxidase DNA release (Fig. 3d).

Mitochondrial electron transport chain complex V inhibitor showed antiviral activity against CVB3 *in vitro*.

Man B is known to inhibit complex I and V of mitochondrial respiratory chain complex I²⁹. Thus, we hypothesised that the antiviral activity of Man B toward CVB3 might be associated with mROS production by inhibition of the mitochondrial respiratory chain complex. Thus, we assessed whether other electron transport chain complex inhibitors, including rotenone (complex I inhibitor), antimycin A (complex III inhibitor), potassium cyanide (complex IV inhibitor), or oligomycin (complex V inhibitor), might have antiviral activity toward CVB3 *in vitro*. Rotenone showed about 20% cytotoxicity at a concentration of 2 μ g/mL; however, antimycin A, potassium cyanide, and oligomycin did not reveal any cytotoxicity at the same concentration. Furthermore, rotenone, antimycin A, and potassium cyanide did not show antiviral activity at concentrations of 0.08, 0.4, and 2 μ g/mL. Only oligomycin showed significant antiviral activity by preventing CVB3-induced cytotoxicity of Vero cells at each concentration (Fig. 4a–d). In addition, co-treatment with Man B and oligomycin did not result in additional antiviral activity compared with that of Man B or oligomycin alone (Supplementary Fig. S6). According to these data, the antiviral activity of Man B could be associated with the inhibition of electron transfer chain complex V but not complex I.

Man B triggered the STING/TBK-1/IRF3 signalling pathway in CVB3-infected cells.

Cytosolic mtDNA can be recognised by cyclic GMP–AMP synthase (cGAS), thus possibly resulting in activation of the STING/TBK-1/IRF3 pathway, which is critical for the expression of antiviral genes^{30,31}. Immunoblotting analysis of STING, p-STING, TBK-1, p-TBK-1, IRF-3, and p-IRF-3 in comparison with β -actin suggested that the expression levels of STING and IRF-3 were significantly increased by Man B treatment in both control and CVB3-infected cells. Furthermore, the levels of STING and TBK-1 phosphorylation were highly increased, suggesting that Man B activated the STING/TBK-1/IRF3 pathway for successful antiviral defence against CVB3 in infected cells (Fig. 5a,b).

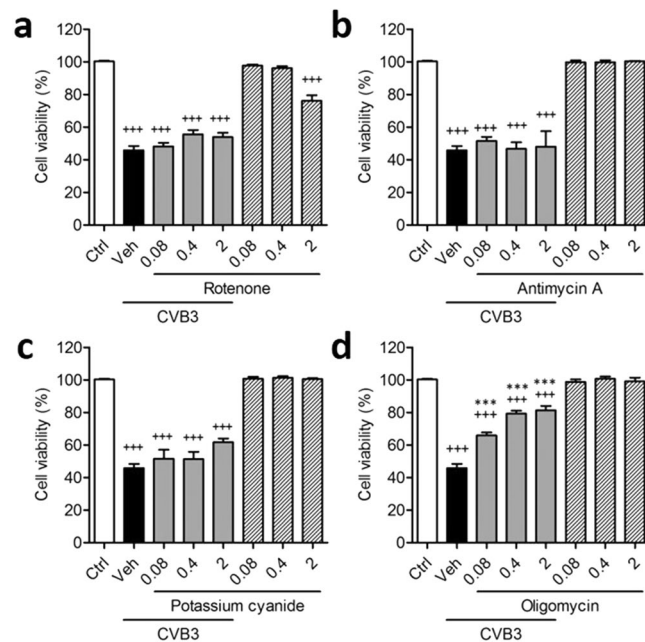


Figure 4. Antiviral activity of mitochondrial electron transport chain complex inhibitors against coxsackievirus B3 *in vitro*. Electron transport chain complex inhibitors rotenone (complex I inhibitor), antimycin A (complex III inhibitor), potassium cyanide (complex IV inhibitor), and oligomycin (complex V inhibitor) were evaluated for their antiviral activity against coxsackievirus B3 (CVB3) in Vero cells. Vero cells were infected with CVB3 in the presence or absence of 0.08, 0.4, and 2 $\mu\text{g}/\text{mL}$ of (a) rotenone, (b) antimycin A, (c) potassium cyanide, or (d) oligomycin for 48 h. Data are presented as means \pm SEM of 3 independent experiments. $+++P < 0.001$ for comparison with non-infected control group (Ctrl); $***P < 0.001$ for comparison with CVB3-infected vehicle group (Veh), Bonferroni's multiple comparison test (ANOVA).

Discussion

Although a variety of pharmacological activities associated with *S. chinensis* have been demonstrated^{13,14,32}, antiviral activities of *S. chinensis* toward coxsackieviruses have not been reported. In this study, we isolated and characterised Man B from *S. chinensis* and demonstrated its strongly antiviral activity against CVB3.

Currently, the prevention and treatment of coxsackievirus infection are limited. A vaccine to prevent coxsackievirus infection is difficult to produce because there are many immunologically non-cross-reactive serotypes. Ribavirin, a broad-spectrum nucleoside analogue, exhibited expected antiviral action. This antiviral drug was previously shown to have an inhibitory effect on many DNA and RNA viruses in cell culture³³. However, ribavirin showed only a marginal effect on CVB3 infection of Vero cells. Further, viruses that had acquired resistance to ribavirin were isolated from several virus populations and observed in some patients³⁴. Therefore, the existence of ribavirin-resistant viruses suggests that development of a novel antiviral drug may be especially important to treat coxsackievirus infection.

In the current study, we found that Man B exhibited strong antiviral activity against coxsackieviruses with IC_{50} values ranging from 0.88 to 8.20 $\mu\text{g}/\text{mL}$. The cytotoxicity of Man B against Vero cells was not observed up to 10 $\mu\text{g}/\text{mL}$, suggesting that Man B is not cytotoxic below 10 $\mu\text{g}/\text{mL}$. Although significant toxicity was not found in mice after four consecutive daily treatments of Man B (2.5 mg/kg/day), the toxicity should be carefully tested in animal models to ensure that Man B is safe *in vivo*.

A recent study showed that CVB3 infection in resistant C57BL/6 mice led to rapid elimination of virus in the heart as a result of enhanced mROS, which might be due to alteration of the mitochondrial respiratory chain³⁵. However, at the cellular level, C3 (pro) cysteine protease of CVB3 cleaved MAVS and TRIF to inhibit type I IFN cytokine production, and consequently, CVB3 infection did not induce a significant type I IFN response in HEK293, HeLa, and Caco-2 cells^{36,37}. MAVS, which is localised in the mitochondrial membrane, is a downstream adaptor molecule that transfers signals for activation of RIG-I, and several viruses including CVB3 employ strategies to disrupt MAVS-dependent antiviral pathways³⁷.

Several studies have shown that ROS generation is linked to the regulation of antiviral signalling as well as mitochondrial homeostasis and apoptotic cell death³⁸. RIG-I-like receptor (RLR) signalling for the recognition of viral infection is dependent on mROS level³⁹. Interestingly, several mitochondrial resident molecules including MAVS might converge with mROS levels for successful IFN signalling^{40,41}. Indeed, a recent study showed that one of the mitochondrial electron transport molecules composing complex IV, cytochrome C oxidase complex subunit 5B (COX5B), physically interacts with MAVS and inhibits MAVS signalling by repressing mROS. In addition, COX5B appears to coordinate with autophagy to negatively regulate MAVS-dependent antiviral signalling³⁸.

Man B was identified as a specific inhibitor of mitochondrial respiratory chain complex I through phenotypic screening using zebrafish embryos²⁹. Biochemical assay suggested that the IC_{50} value of Man B for complex I

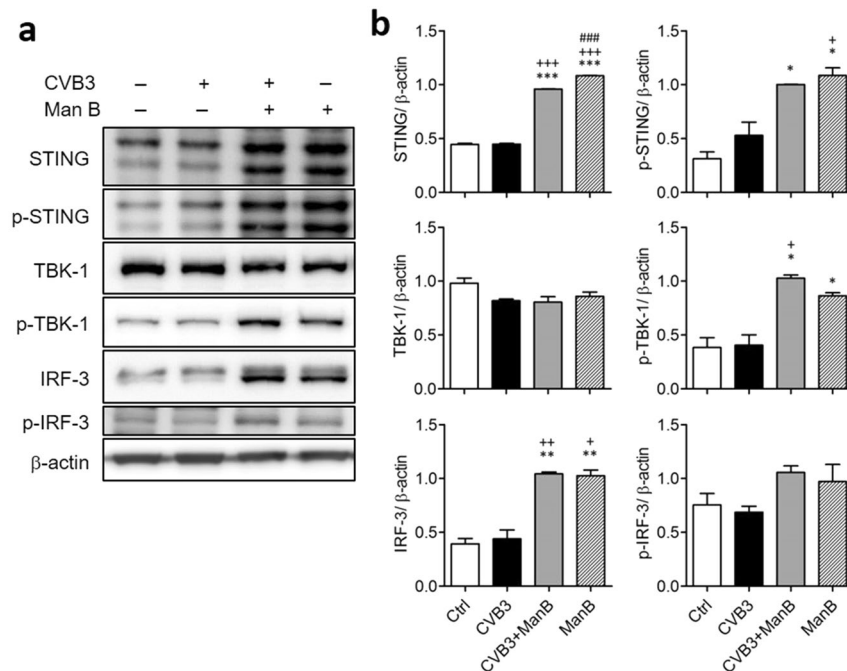


Figure 5. Manassantin B induced STING/TBK-1 signalling in coxsackievirus B3-infected cells. **(a)** Representative immunoblot of STING, p-STING, TBK-1, p-TBK-1, IRF-3, p-IRF-3, and β -actin to evaluate activation of their expression in coxsackievirus B3 (CVB3)-infected Vero cells or uninfected cells after treatment with manassantin B (Man B) (2 μ g/mL). The samples were derived from the same experiment, and gels/blots were processed in parallel. **(b)** Density of western blot bands was calculated as the relative expression of STING, p-STING, TBK-1, p-TBK-1, IRF-3, and p-IRF-3. Each band was normalised by the density of the β -actin band. Data are presented as means \pm SEM of 3 independent experiments. * P < 0.05, ** P < 0.01, *** P < 0.001 for comparison with non-infected control group (Ctrl); + P < 0.05, ++ P < 0.01, +++ P < 0.001 for comparison with CVB3-infected vehicle group; ### P < 0.001 for comparison with CVB3-infected Man B group, Bonferroni's multiple comparison test (ANOVA).

inhibition was less than 25 nM and that Man B shares some mechanistic characteristics with rotenone²⁹. Although treatment of cells with rotenone induced apoptotic cell death by inhibiting mitochondrial complex I, HIV-1-infected cells were insensitive to rotenone-induced cell death, suggesting that mitochondrial complex I might be downregulated, or mROS generation might be blocked by some viral infection such as HIV-1 infection⁴². Likewise, we found that treatment of Vero cells with CVB3 slightly but not significantly inhibited mROS generation as compared with that of control cells treated with vehicle only (Fig. 3b).

Although CVB3 infection alone did not induce mROS production in Vero cells, treatment with Man B significantly increased mROS production. Since mROS is closely associated with mitochondrial damage⁴³, we presume that Man B can induce mtDNA release into the cytosol, which may activate cGAS to generate cyclic dinucleotide cyclic-GMP-AMP (cGAMP) as a secondary messenger⁴⁴. The increase in cGAMP triggers kinase activity of STING and transduces p-IRF3/IRF3 signalling to switch on antiviral transcription in nuclei of infected cells⁴⁵. In our study, CVB3-infected cells did not activate IRF-3 phosphorylation; however, Man B treatment of those cells significantly induced the phosphorylation of TBK-1 and IRF-3 to activate antiviral gene expression, which was inhibited by CVB3 (Fig. 6).

In the current study, we showed that Man B inhibited the replication of CVB3 by activating the STING/TBK-1/IRF3 pathway as well as increasing mitochondrial ROS. Recently, cGAS cytosolic DNA was implicated in the viral sensing pathways including the STING/TBK-1/IRF3 pathway via G3BP1^{46,47}. Because G3BP1-eIF4G1, which is important for stress granule formation, was reported as a target of picornavirus proteases^{48,49}, it would be interesting to evaluate whether the antiviral activity of Man B is associated with the regulation of G3BP1.

Thus, our results suggest that the antiviral activity induced by Man B treatment was associated with production of mROS and activation of type I IFN signalling through activation of the cGAS/STING/TBK-1/IRF3 pathway. In the future, we will continue evaluating whether such strategy is applicable for the development of antiviral drugs and identifying antiviral drug candidates through screening of compounds that induce mitochondrial damage.

Methods

Extraction and isolation of active compounds from *S. chinensis* Baill. Aerial portions of *S. chinensis* Baill were purchased at Gyeongsangnamdo Agricultural Research & Extension Services, Korea, in November 2009. The dried, ground plants (1.2 kg) were finely powdered with a blender, after which the powder was macerated in 3 L of methanol at room temperature for 3 days. Then, the macerate was filtered (Whatman No. 2), and the process was repeated three times. The combined filtrates were evaporated using a 40 °C water bath to

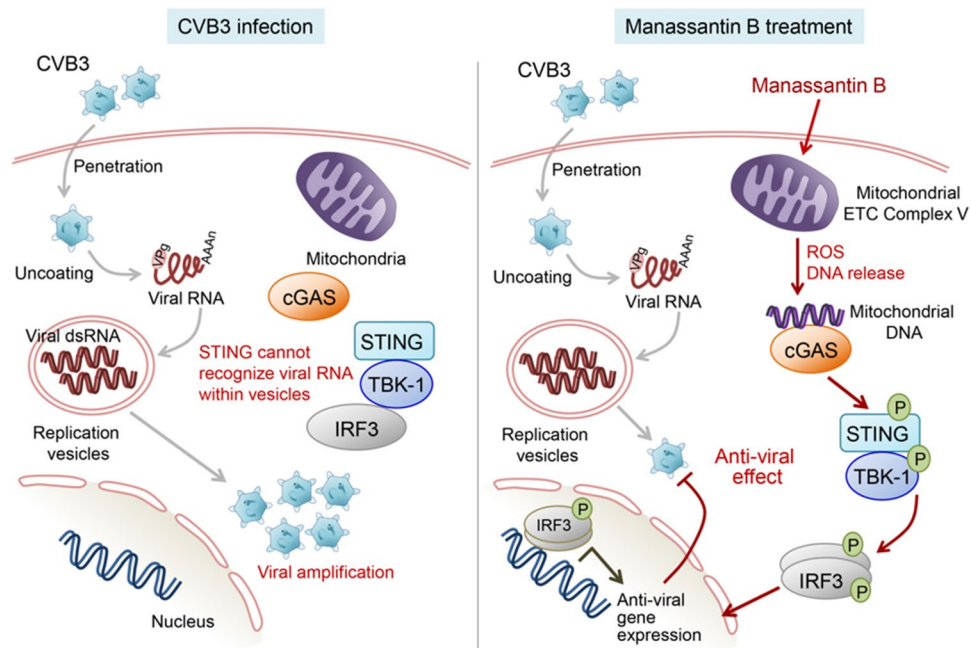


Figure 6. Proposed mechanism for antiviral activity of manassantin B toward coxsackievirus B3. Once coxsackievirus B3 (CVB3) infects host cells, virus particles are uncoated from their capsid protein and subsequently release viral RNA into the cytosol. Because viral replication occurs inside replication vesicles such as intracellular organelles, host pattern-associated molecular pattern sensor proteins, such as cGAS and MAVS, cannot adequately recognise their counterpart ligand. When manassantin B is administered to CVB3-infected cells, it can suppress mitochondrial electron transport chain (ETC) complex 1 and 5. Suppressed ETC results in increased mitochondrial ROS production and shutdown of mitochondrial function. In addition, mitochondria suppressed by manassantin B release their own DNA, which may be recognised by cGAS. Mitochondrial DNA-recognised cGAS synthesises cGAMP, which serves as a secondary messenger, by conjugating ATP and GTP. cGAMP binds with STING, resulting in STING activation and TBK-1 recruitment. Phosphorylated TBK-1 phosphorylates IRF-3, which dimerises, is imported into the nucleus, and serves as a transcription factor for antiviral gene expression. Finally, viral replication can be suppressed by antiviral gene expression, which is activated by manassantin B.

produce (yield) 84.2 g of a dark green residue. The methanol extract (84.2 g) was dissolved in 1 L of water and then separated with *n*-hexane, ethyl acetate, and *n*-butanol, respectively. The ethyl acetate-soluble extract was evaporated under reduced pressure to yield 30.07 g of residue. Next, the ethyl acetate-soluble extract (30.07 g) was subjected to C_{18} column chromatography (40–63 μ m, 300 g; Merck, Kenilworth, NJ, USA) and eluted with a gradient consisting of methanol:water (2:8, 4:6, 6:4, 8:2, 10:0; 2×500 mL each). Fractions of similar pattern were pooled to produce 10 fractions (Fr.1–Fr.10) on the basis of thin layer chromatography analysis. Based on the bioassay-guided fractionation, Fr.10 showed the most potent inhibitory effects against CVB3 (Supplementary Tables S1 and S2). Furthermore, Fr.10 was purified by preparative reversed-phase HPLC using a gradient of 30%–100% acetonitrile in water (Capcell Pak C18 UG120, 250×10 mm, 10 μ m; Shisheido, Tokyo, Japan) to obtain Man B. The structures of active compounds were determined by spectroscopic analysis, including EI-MS, 1 H-NMR, and 13 C-NMR (Supplementary Fig. S1).

Cell lines, viruses, and reagents. CVB3 (ATCC VR-30) was obtained from American Type Culture Collection (Manassas, VA, USA) and propagated at 37 °C in Vero cells maintained in minimal essential medium supplemented with 10% (v/v) foetal bovine serum (FBS) and 1% (v/v) antibiotic–antimycotic solution. Gibco® antibiotic–antimycotic solution, trypsin-ethylenediamine tetraacetic acid, FBS, and minimal essential medium were purchased from Life Technologies (Carlsbad, CA, USA), and Falcon™ tissue culture plates were purchased from BD Biosciences (San Jose, CA, USA). Rotenone, antimycin A, potassium cyanide, and oligomycin were purchased from Sigma–Aldrich (St. Louis, MO, USA), and ribavirin was obtained from Duchefa Biochemie (Haarlem, The Netherlands).

Antiviral activity assay. The day before infection, 3×10^4 Vero cells/well were seeded onto a 96-well culture plate. The next day, the culture medium was aspirated, and the cells were washed with $1 \times$ PBS. Then, 0.09 mL of the diluted virus suspension containing the virus stock at a multiplicity of infection (MOI) of 0.8 with 1% FBS added to produce an appropriate cytopathic effect (CPE) within 2 days after infection, followed by the addition of 0.01 mL of test compound. The test compounds were prepared by a 10-fold dilution scheme. The antiviral activity of each test compound was determined with four concentrations ranging from 0.1 μ g/mL to 10 μ g/mL. We used three wells each for virus controls (virus-infected, non-drug-treated cells) and cell controls (non-infected,

non-drug-treated cells). The 96-well culture plates were incubated at 37 °C in 5% CO₂ for 2–3 days until 70%–80% CPE. To prevent false-positive results due to the presence of dead cells in the sulforhodamine B (SRB) assay, we discarded the supernatant and thoroughly washed the wells with PBS twice at the end of culture. Then, cells were fixed with ice-cold 70% acetone (100 µL/well) for 30 min at –20 °C and stained with 0.4% SRB in 1% acetic acid. SRB-stained cells were solubilised with 10 mM unbuffered Tris base solution, and the absorbance was measured at 562 nm using a SpectraMax® i3 microplate reader (Molecular Devices, Palo Alto, CA, USA) with a reference absorbance of 620 nm. The results were then transformed into percentages of the controls, and the percent protection achieved by the test compound in the virus-infected cells was calculated using the following formula: $[(OD_{\text{virus}} - (OD_{\text{virus}})_{\text{mock}}) \div ((OD_{\text{virus}})_{\text{mock}} - (OD_{\text{virus}})_{\text{virus}}) \times 100\%$, where $(OD_{\text{virus}})_{\text{virus}}$ is the optical density measured with a given concentration of the test compound in virus-infected cells; $(OD_{\text{virus}})_{\text{virus}}$ is the optical density of the non-drug-treated, virus-infected control cells; and $(OD_{\text{virus}})_{\text{mock}}$ is the optical density.

PCR analysis. Vero cells in culture plates were tested when confluent. The culture medium was removed, and the cells were washed with PBS. Then, 90 µL of diluted virus suspension and 10 µL of medium supplemented with 1% FBS containing active compounds were added. The 96-well culture plates were incubated at 37 °C in 5% CO₂ for 48–72 h until 70%–80% CPE. Cells exhibiting 70% CPE were frozen and thawed three times, and viral RNA was extracted from the infected cells using the QIAamp Viral RNA Mini kit (Qiagen, Hilden, Germany)⁵⁰. cDNA was generated in a 20-µL reaction for 30 min at 42 °C using 1 µg RNA, random primers, and SuperScript II reverse transcriptase (Invitrogen) according to the manufacturer's instructions⁵⁰. RT-PCR was performed with a GeneAmp PCR System 2700 (Perkin-Elmer/Cetus, Norwalk, CT, USA) using primer sets specific for the 5' NCR of the enterovirus and β-actin⁵¹ of Vero cells. Briefly, a 50-µL reaction mixture containing 0.2 µM of ENT-F and ENT-R⁵² or β-actin primers⁵³, 2 U of Taq DNA polymerase (Promega, Madison, WI, USA), 100 µM dNTPs, and 2 µM MgCl₂ was subjected to 35 cycles of 94 °C for 1 min, 52 °C for 1 min, and 72 °C for 1 min. The final extension step was extended to 72 °C for 7 min⁵⁴. PCR-amplified products were separated on 1.5% agarose gels containing 0.1 µg/mL ethidium bromide and visualised under UV light.

Quantitative real-time PCR was conducted with 1 µL of cDNA. A customised AccuPower® Enterovirus Real Time RT-PCR Kit (Bioneer Corp., Daejeon, South Korea) and QuantStudio 5 system (Thermo Fisher Scientific, Waltham, MA, USA) were used for quantification under the following conditions: 10 min at 95 °C for initial denaturation, followed by 45 cycles of amplification with denaturation at 95 °C for 15 s and annealing/extension at 55 °C for 30 s. A standard curve was generated using 10-fold serial dilutions (10⁹ to 10³ copies/test) of *in vitro*-synthesised RNA strands.

Western blotting. Rabbit anti-cytoskeletal actin (Bethyl Laboratories, Montgomery, TX, USA), mouse anti-CVB3 VP1 (Dako, Copenhagen, Denmark), mouse anti-α tubulin (Santa Cruz Biotechnology, Dallas, TX, USA), rabbit anti-STING, rabbit anti-phospho-STING (Ser336), rabbit anti-TBK-1, rabbit anti-phospho-TBK-1 (Ser172), rabbit anti-IRF-3, and rabbit anti-phospho-IRF-3 (Ser396) (all from Cell Signaling Technologies, Danvers, MA, USA) antibodies were used. The enhanced chemiluminescence substrate femto LUCENT™ PLUS-HRP (G-Biosciences, St. Louis, MO, USA) was applied, and images of bands were captured using an Image Quant™ LAS 4000 Mini system (GE Healthcare Life Sciences, Little Chalfont, UK). Quantification of band densities was performed using ImageJ software (NIH, Bethesda, MD, USA).

mROS measurement. Vero cells (1 × 10⁶) were seeded onto a 6-well plate. The next day, the supernatant of each well was replaced with viral infection media or fresh media with Man B. After 4 h, cells were harvested by trypsinisation and stained with MitoSox Red (Invitrogen) mitochondrial superoxide indicator according to the manufacturer's guideline. Stained cells were analysed via FACSVerse (BD Biosciences) without the formalin fixation step.

mtDNA detection in cytosolic fraction. After no treatment, CBV3 infection, CBV3 infection and Man B treatment, or Man B treatment only, 2 × 10⁶ Vero cells were harvested. Each cell suspension was equally divided into two aliquots. One aliquot was used for extraction of the cytosolic fraction with the Mitochondria/Cytosol fractionation kit (Enzo Life Sciences, Farmingdale, NY, USA). The other aliquot was used for genomic DNA extraction via the QIAamp DNA Blood Mini Kit (Qiagen). To quantify mtDNA in the cytosolic fraction, real-time PCR was performed with cytochrome C oxidase primers. Cytosolic cytochrome C oxidase amplification was normalised by β-actin amplification of whole genomic DNA.

Animal model. Female BALB/c mice aged 4 weeks were purchased from SPL Laboratory Animal Company (Koatech Bio, Pyeongtaek, Korea). All mice were maintained under specific pathogen-free conditions for 1 week in the experimental facilities at Kangwon National University (Chuncheon, Korea), where they received sterilised food and water *ad libitum* and were housed at 20–22 °C with a 12-hours light/dark cycle. All animal experiments were performed in accordance with guidelines set and approved by the Institutional Animal Care and Use Committees of Kangwon National University (KW-161101-2). Five-week-old female BALB/c mice were intraperitoneally inoculated with 1 × 10⁶ pfu/mouse of CVB3. BALB/C mice infected with CVB3 were orally administered Man B (2.5 mg/kg/day) or ribavirin (10 mg/kg/day) for 4 days²⁷.

Cytokine and chemokine assay. We confirmed the level of cytokines and chemokines with ELISA kits for TNF-α, IL-6, IFN-γ, CCL2 (MCP1) (all from eBioscience, San Diego, CA, USA), and KC (CXCL1) (R&D Systems, Minneapolis, MN, USA). Serum was obtained as previously described⁵⁵. Lungs were obtained from mice infected with CVB3, and the same amount of lung tissue was homogenised to obtain supernatants. The cytokine and chemokine levels in lung supernatant were evaluated according to the manufacturer's instructions²⁵. The absorbance was then read at 450 nm using a SpectraMax 340 (Molecular Devices).

Statistical analysis. We used Student's *t*-test to compare the differences between two groups. To compare multiple groups, we performed one-way ANOVA followed by Bonferroni's multiple comparison test. Values of $P < 0.05$ were considered significant at a 95% confidence interval.

References

- Zell, R. *et al.* ICTV Virus Taxonomy Profile: Picornaviridae. *The Journal of general virology* **98**, 2421–2422, <https://doi.org/10.1099/jgv.0.000911> (2017).
- Bendig, J. W. *et al.* Coxsackievirus B3 sequences in the blood of a neonate with congenital myocarditis, plus serological evidence of maternal infection. *Journal of medical virology* **70**, 606–609, <https://doi.org/10.1002/jmv.10437> (2003).
- Fujioka, S. *et al.* Evaluation of viral infection in the myocardium of patients with idiopathic dilated cardiomyopathy. *Journal of the American College of Cardiology* **36**, 1920–1926 (2000).
- Spanakis, N. *et al.* Coxsackievirus B3 sequences in the myocardium of fatal cases in a cluster of acute myocarditis in Greece. *Journal of clinical pathology* **58**, 357–360, <https://doi.org/10.1136/jcp.2004.020099> (2005).
- Filippi, C. M. & von Herrath, M. G. Viral trigger for type 1 diabetes: pros and cons. *Diabetes* **57**, 2863–2871, <https://doi.org/10.2337/db07-1023> (2008).
- Drescher, K. M., Kono, K., Bopegamage, S., Carson, S. D. & Tracy, S. Coxsackievirus B3 infection and type 1 diabetes development in NOD mice: insulinitis determines susceptibility of pancreatic islets to virus infection. *Virology* **329**, 381–394, <https://doi.org/10.1016/j.virol.2004.06.049> (2004).
- Wu, K. X., Ng, M. M. & Chu, J. J. Developments towards antiviral therapies against enterovirus 71. *Drug discovery today* **15**, 1041–1051, <https://doi.org/10.1016/j.drudis.2010.10.008> (2010).
- Vlietinck, A. J. & Vanden Berghe, D. A. Can ethnopharmacology contribute to the development of antiviral drugs? *Journal of ethnopharmacology* **32**, 141–153 (1991).
- Cowan, M. M. Plant products as antimicrobial agents. *Clinical microbiology reviews* **12**, 564–582 (1999).
- Briskin, D. P. Medicinal plants and phytomedicines. Linking plant biochemistry and physiology to human health. *Plant physiology* **124**, 507–514 (2000).
- Williams, J. E. Review of antiviral and immunomodulating properties of plants of the Peruvian rainforest with a particular emphasis on Una de Gato and Sangre de Grado. *Alternative medicine review: a journal of clinical therapeutics* **6**, 567–579 (2001).
- Jassim, S. A. & Naji, M. A. Novel antiviral agents: a medicinal plant perspective. *Journal of applied microbiology* **95**, 412–427 (2003).
- Rao, K. V. & Rao, N. S. Chemistry of *Saururus cernuus*, VI: Three new neolignans. *Journal of natural products* **53**, 212–215 (1990).
- Jeong, H. J. *et al.* Inhibitory effects of *Saururus chinensis* and its components on stomach cancer cells. *Phytomedicine: international journal of phytotherapy and phytopharmacology* **22**, 256–261, <https://doi.org/10.1016/j.phymed.2014.12.003> (2015).
- Seo, C. S. *et al.* Protective effect of lignans against sepsis from the roots of *Saururus chinensis*. *Biological & pharmaceutical bulletin* **31**, 523–526 (2008).
- Rao, K. V., Puri, V. N., Diwan, P. K. & Alvarez, F. M. Preliminary evaluation of manassantin A, a potential neuroleptic agent from *Saururus cernuus*. *Pharmacological research communications* **19**, 629–638 (1987).
- Sung, S. H. & Kim, Y. C. Hepatoprotective diastereomeric lignans from *Saururus chinensis* herbs. *Journal of natural products* **63**, 1019–1021 (2000).
- Kubaneck, J., Fenical, W., Hay, M. E., Brown, P. J. & Lindquist, N. Two antifedant lignans from the freshwater macrophyte *Saururus cernuus*. *Phytochemistry* **54**, 281–287 (2000).
- Rho, M. C. *et al.* Inhibitory effects of manassantin A and B isolated from the roots of *Saururus chinensis* on PMA-induced ICAM-1 expression. *Planta medica* **69**, 1147–1149, <https://doi.org/10.1055/s-2003-818007> (2003).
- Hwang, B. Y., Lee, J. H., Nam, J. B., Hong, Y. S. & Lee, J. J. Lignans from *Saururus chinensis* inhibiting the transcription factor NF- κ B. *Phytochemistry* **64**, 765–771 (2003).
- Lee, J. H. *et al.* Suppression of RelA/p65 transactivation activity by a lignoid manassantin isolated from *Saururus chinensis*. *Biochemical pharmacology* **66**, 1925–1933 (2003).
- Lee, W. S. *et al.* Human ACAT-1 and -2 inhibitory activities of saucerneol B, manassantin A and B isolated from *Saururus chinensis*. *Bioorganic & medicinal chemistry letters* **14**, 3109–3112, <https://doi.org/10.1016/j.bmcl.2004.04.023> (2004).
- Rao, K. V. & Reddy, G. C. Chemistry of *Saururus cernuus*, V. sauristolactam and other nitrogenous constituents. *Journal of natural products* **53**, 309–312 (1990).
- Hwang, B. Y. *et al.* Sauchinone, a lignan from *Saururus chinensis*, suppresses iNOS expression through the inhibition of transactivation activity of RelA of NF- κ B. *Planta medica* **69**, 1096–1101, <https://doi.org/10.1055/s-2003-45189> (2003).
- Seo, S. U. *et al.* Type I interferon signaling regulates Ly6C(hi) monocytes and neutrophils during acute viral pneumonia in mice. *PLoS pathogens* **7**, e1001304, <https://doi.org/10.1371/journal.ppat.1001304> (2011).
- Kang, H. *et al.* Synergistic antiviral activity of gencitabine and ribavirin against enteroviruses. *Antiviral research* **124**, 1–10, <https://doi.org/10.1016/j.antiviral.2015.10.011> (2015).
- Kwon, B. E. *et al.* Antiviral Activity of Oroxylin A against Coxsackievirus B3 Alleviates Virus-Induced Acute Pancreatic Damage in Mice. *PLoS one* **11**, e0155784, <https://doi.org/10.1371/journal.pone.0155784> (2016).
- West, A. P. *et al.* Mitochondrial DNA stress primes the antiviral innate immune response. *Nature* **520**, 553–557, <https://doi.org/10.1038/nature14156> (2015).
- Lai, K. *et al.* Integrated compound profiling screens identify the mitochondrial electron transport chain as the molecular target of the natural products manassantin, sesquicillin, and arctigenin. *ACS chemical biology* **8**, 257–267, <https://doi.org/10.1021/cb300495e> (2013).
- Riley, J. S. *et al.* Mitochondrial inner membrane permeabilisation enables mtDNA release during apoptosis. *The EMBO journal* **37**, <https://doi.org/10.15252/embj.201899238> (2018).
- Franz, K. M., Neidermyer, W. J., Tan, Y. J., Whelan, S. P. J. & Kagan, J. C. STING-dependent translation inhibition restricts RNA virus replication. *Proceedings of the National Academy of Sciences of the United States of America* **115**, E2058–e2067, <https://doi.org/10.1073/pnas.1716937115> (2018).
- Oh, K. S. *et al.* Cardiovascular effects of lignans isolated from *Saururus chinensis*. *Planta medica* **74**, 233–238, <https://doi.org/10.1055/s-2008-1034310> (2008).
- Choi, H. J., Song, H. H., Lee, J. S., Ko, H. J. & Song, J. H. Inhibitory Effects of Norwogonin, Oroxylin A, and Mosloflavone on Enterovirus 71. *Biomolecules & therapeutics* **24**, 552–558, <https://doi.org/10.4062/biomolther.2015.200> (2016).
- Graci, J. D. & Cameron, C. E. Mechanisms of action of ribavirin against distinct viruses. *Reviews in medical virology* **16**, 37–48, <https://doi.org/10.1002/rmv.483> (2006).
- Ebermann, L. *et al.* The mitochondrial respiratory chain has a critical role in the antiviral process in Coxsackievirus B3-induced myocarditis. *Laboratory investigation; a journal of technical methods and pathology* **92**, 125–134, <https://doi.org/10.1038/labinvest.2011.145> (2012).
- Mukherjee, A. *et al.* The coxsackievirus B3 protease cleaves MAVS and TRIF to attenuate host type I interferon and apoptotic signaling. *PLoS pathogens* **7**, e1001311, <https://doi.org/10.1371/journal.ppat.1001311> (2011).
- Feng, Q. *et al.* Enterovirus 2Apro targets MDA5 and MAVS in infected cells. *Journal of virology* **88**, 3369–3378, <https://doi.org/10.1128/jvi.02712-13> (2014).

38. Zhao, Y. *et al.* COX5B regulates MAVS-mediated antiviral signaling through interaction with ATG5 and repressing ROS production. *PLoS pathogens* **8**, e1003086, <https://doi.org/10.1371/journal.ppat.1003086> (2012).
39. Tal, M. C. *et al.* Absence of autophagy results in reactive oxygen species-dependent amplification of RLR signaling. *Proceedings of the National Academy of Sciences of the United States of America* **106**, 2770–2775, <https://doi.org/10.1073/pnas.0807694106> (2009).
40. Bender, S. *et al.* Activation of Type I and III Interferon Response by Mitochondrial and Peroxisomal MAVS and Inhibition by Hepatitis C Virus. *PLoS pathogens* **11**, e1005264, <https://doi.org/10.1371/journal.ppat.1005264> (2015).
41. Agod, Z. *et al.* Regulation of type I interferon responses by mitochondria-derived reactive oxygen species in plasmacytoid dendritic cells. *Redox biology* **13**, 633–645, <https://doi.org/10.1016/j.redox.2017.07.016> (2017).
42. Ladha, J. S., Tripathy, M. K. & Mitra, D. Mitochondrial complex I activity is impaired during HIV-1-induced T-cell apoptosis. *Cell death and differentiation* **12**, 1417–1428, <https://doi.org/10.1038/sj.cdd.4401668> (2005).
43. Sena, L. A. & Chandel, N. S. Physiological roles of mitochondrial reactive oxygen species. *Molecular cell* **48**, 158–167, <https://doi.org/10.1016/j.molcel.2012.09.025> (2012).
44. Wu, J. *et al.* Cyclic GMP-AMP is an endogenous second messenger in innate immune signaling by cytosolic DNA. *Science (New York, N.Y.)* **339**, 826–830, <https://doi.org/10.1126/science.1229963> (2013).
45. Liu, S. *et al.* Phosphorylation of innate immune adaptor proteins MAVS, STING, and TRIF induces IRF3 activation. *Science (New York, N.Y.)* **347**, aaa2630, <https://doi.org/10.1126/science.aaa2630> (2015).
46. Wisner, C., Kim, B. & Ascano, M. G3BP1 enhances cytoplasmic DNA pattern recognition. *Nature immunology* **20**, 5–7, <https://doi.org/10.1038/s41590-018-0279-8> (2019).
47. Liu, Z. S. *et al.* G3BP1 promotes DNA binding and activation of cGAS. *Nature immunology* **20**, 18–28, <https://doi.org/10.1038/s41590-018-0262-4> (2019).
48. Yang, X. *et al.* SG formation relies on eIF4G1-G3BP interaction which is targeted by picornavirus stress antagonists. *Cell discovery* **5**, 1, <https://doi.org/10.1038/s41421-018-0068-4> (2019).
49. Dougherty, J. D., Tsai, W. C. & Lloyd, R. E. Multiple Poliovirus Proteins Repress Cytoplasmic RNA Granules. *Viruses* **7**, 6127–6140, <https://doi.org/10.3390/v7122922> (2015).
50. Li, L. *et al.* Genetic characteristics of human enterovirus 71 and coxsackievirus A16 circulating from 1999 to 2004 in Shenzhen, People's Republic of China. *Journal of clinical microbiology* **43**, 3835–3839, <https://doi.org/10.1128/jcm.43.8.3835-3839.2005> (2005).
51. Kuo, Y. C., Chen, C. C., Tsai, W. J. & Ho, Y. H. Regulation of herpes simplex virus type 1 replication in Vero cells by Psychotria serpens: relationship to gene expression, DNA replication, and protein synthesis. *Antiviral research* **51**, 95–109 (2001).
52. Zoll, G. J. *et al.* General primer-mediated polymerase chain reaction for detection of enteroviruses: application for diagnostic routine and persistent infections. *Journal of clinical microbiology* **30**, 160–165 (1992).
53. Cone, R. W., Hobson, A. C., Palmer, J., Remington, M. & Corey, L. Extended duration of herpes simplex virus DNA in genital lesions detected by the polymerase chain reaction. *The Journal of infectious diseases* **164**, 757–760 (1991).
54. Baek, K. *et al.* Epidemics of enterovirus infection in Chungnam Korea, 2008 and 2009. *Virology journal* **8**, 297, <https://doi.org/10.1186/1743-422x-8-297> (2011).
55. Seo, S. U. *et al.* MyD88 signaling is indispensable for primary influenza A virus infection but dispensable for secondary infection. *Journal of virology* **84**, 12713–12722, <https://doi.org/10.1128/jvi.01675-10> (2010).

Acknowledgements

This study was supported by the National Research Foundation of Korea (NRF) funded by the Ministry of Science, ICT and Future Planning and Ministry of Education (grant numbers NRF-2017M3A9C8060390, NRF-2017R1A2B2001963, NRF-2016R1A6A3A11932323) and the Korea Health Technology R&D Project through the Korea Health Industry Development Institute (KHIDI), funded by the Ministry of Health & Welfare, Republic of Korea (grant number HI15C1980). This study was performed with the support of a research grant of Kangwon National University in 2017.

Author Contributions

J.H.S. and J.H.A. conducted most of the experiments. S.R.K., E.H.H., D.K., M.C., Y.C., and B.E.K. contributed to some experiments. S.C. and H.J.C. analyzed the data. J.H.S. and J.H.A. wrote the manuscript. S.Y.C. and H.J.K. designed the experiments and wrote the manuscript.

Additional Information

Supplementary information accompanies this paper at <https://doi.org/10.1038/s41598-019-45868-8>.

Competing Interests: The authors declare no competing interests.

Publisher's note: Springer Nature remains neutral with regard to jurisdictional claims in published maps and institutional affiliations.



Open Access This article is licensed under a Creative Commons Attribution 4.0 International License, which permits use, sharing, adaptation, distribution and reproduction in any medium or format, as long as you give appropriate credit to the original author(s) and the source, provide a link to the Creative Commons license, and indicate if changes were made. The images or other third party material in this article are included in the article's Creative Commons license, unless indicated otherwise in a credit line to the material. If material is not included in the article's Creative Commons license and your intended use is not permitted by statutory regulation or exceeds the permitted use, you will need to obtain permission directly from the copyright holder. To view a copy of this license, visit <http://creativecommons.org/licenses/by/4.0/>.

© The Author(s) 2019